

NAVAL POSTGRADUATE SCHOOL

Monterey, California



THESIS

RADIATION PATTERNS OF ANTENNAS INSTALLED ON AIRCRAFT

by

James Calusdian

December 1998

Thesis Advisor

David C. Jenn

Approved for public release; distribution is unlimited

DTIC QUALITY INSPECTED 2

19990205 034

REPORT DOCUMENTATION PAGE			Form Approved OMB No. 0704-0188	
Public reporting burden for this collection of information is estimated to average 1 hour per response, including the time for reviewing instruction, searching existing data sources, gathering and maintaining the data needed, and completing and reviewing the collection of information. Send comments regarding this burden estimate or any other aspect of this collection of information, including suggestions for reducing this burden, to Washington Headquarters Services, Directorate for Information Operations and Reports, 1215 Jefferson Davis Highway, Suite 1204, Arlington, VA 22202-4302, and to the Office of Management and Budget, Paperwork Reduction Project (0704-0188) Washington DC 20503.				
1. AGENCY USE ONLY (Leave blank)		2. REPORT DATE December 1998		3. REPORT TYPE AND DATES COVERED Master's Thesis
4. TITLE AND SUBTITLE RADIATION PATTERNS OF ANTENNAS INSTALLED ON AIRCRAFT			5. FUNDING NUMBERS	
6. AUTHOR(S) Calusdian, James				
7. PERFORMING ORGANIZATION NAME(S) AND ADDRESS(ES) Naval Postgraduate School Monterey CA 93943-5000			8. PERFORMING ORGANIZATION REPORT NUMBER	
9. SPONSORING/MONITORING AGENCY NAME(S) AND ADDRESS(ES)			10. SPONSORING/MONITORING AGENCY REPORT NUMBER	
11. SUPPLEMENTARY NOTES The views expressed in this thesis are those of the author and do not reflect the official policy or position of the Department of Defense or the U.S. Government.				
12a. DISTRIBUTION/AVAILABILITY STATEMENT Approved for public release; distribution is unlimited.			12b. DISTRIBUTION CODE	
13. ABSTRACT (maximum 200 words) This thesis presents a study of radiation patterns for low-gain antennas installed on aircraft. With the aid of the computer program APATCH, a simulation of the radiation patterns for a given antenna located at various points on an aircraft structure can be evaluated. The program uses a technique referred to as Shooting and Bouncing Rays (SBR), which is valid for structures that have typical dimensions of ten wavelengths or more. A Cessna 172 aircraft with a quarter-wavelength monopole antenna and an F-18 aircraft with a telemetry antenna are analyzed.				
14. SUBJECT TERMS Radiation Pattern, Antennas, Aircraft, Physical Optics (PO), Geometrical Optics (GO), Shooting-and-Bouncing Rays (SBR), APATCH			15. NUMBER OF PAGES 54	
			16. PRICE CODE	
17. SECURITY CLASSIFI- CATION OF REPORT Unclassified	18. SECURITY CLASSIFI- CATION OF THIS PAGE Unclassified	19. SECURITY CLASSIFICA- TION OF ABSTRACT Unclassified	20. LIMITATION OF ABSTRACT UL	

Approved for public release; distribution is unlimited

RADIATION PATTERNS OF ANTENNAS INSTALLED ON AIRCRAFT

James Calusdian
B.S., California State University, Fresno, 1988

Submitted in partial fulfillment of the
requirements for the degree of

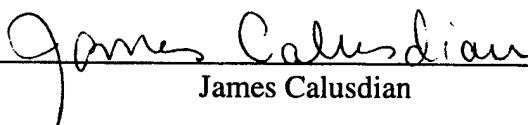
MASTER OF SCIENCE IN ELECTRICAL ENGINEERING

from the

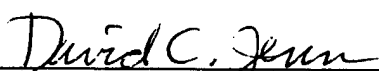
NAVAL POSTGRADUATE SCHOOL

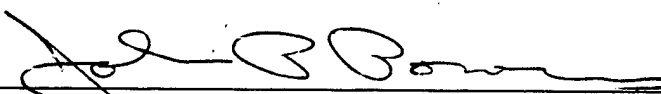
December 1998

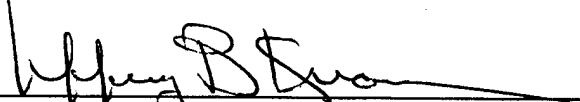
Author:


James Calusdian

Approved by:


David C. Jenn, Thesis Advisor


John P. Powers, Second Reader


Jeffrey B. Knorr, Chairman,
Department of Electrical and Computer Engineering

ABSTRACT

This thesis presents a study of radiation patterns for low-gain antennas installed on aircraft. With the aid of the computer program APATCH, a simulation of the radiation patterns for a given antenna located at various points on an aircraft structure can be evaluated. The program uses a technique referred to as Shooting and Bouncing Rays (SBR), which is valid for structures that have typical dimensions of ten wavelengths or more. A Cessna 172 aircraft with a quarter-wavelength monopole antenna and an F-18 aircraft with a telemetry antenna are analyzed.

TABLE OF CONTENTS

I. INTRODUCTION.....	1
A. OVERVIEW.....	1
B. DETERMINING THE RADIATION PATTERN.....	4
C. THESIS OUTLINE.....	6
II. OVERVIEW OF ELECTROMAGNETIC CONCEPTS.....	7
A. SCATTERING MECHANISMS.....	7
B. SURVEY OF METHODS USED TO SOLVE THE SCATTERING PROBLEM...	8
C. APATCH.....	12
D. PRELIMINARY STUDY.....	14
E. PATCH.....	18
III. AIRCRAFT/ANTENNA SYSTEM EVALUATIONS.....	21
A. CESSNA 172 WITH TCAS ANTENNA.....	21
B. F-18 HORNET WITH TELEMETRY ANTENNA.....	29
IV. SUMMARY AND CONCLUSIONS.....	39
LIST OF REFERENCES.....	41
INITIAL DISTRIBUTION LIST.....	43

ACKNOWLEDGEMENT

The author is very grateful to the Long-Term Full-Time Training program and Edwards AFB which have provided the means for this very unique and rewarding educational opportunity. Also, the author would like to thank all of the outstanding professors and staff at the Naval Postgraduate School for their tutoring and assistance in his learning endeavors. Additionally, the author is very appreciative of the insight and contributions of Professors John P. Powers and Jeffery B. Knorr.

A very special thanks is extended to Professor David C. Jenn. His patience, guidance, and dedication, which he has so graciously put forward, have made possible this work, and many others like it.

I. INTRODUCTION

A. OVERVIEW

During the design of an aircraft, it becomes necessary to establish the location of the various antennas that are required of the avionics systems. These systems provide for a number of functions essential to the operation of the aircraft: communications and navigation, radar, and EW. Communications and navigation functions are accomplished by such systems as UHF/VHF radios, TACAN, ILS, GPS, and radar altimeter. Radar and EW systems are used by the aircrew to fulfill specific offensive and defensive mission objectives. Examples are target identification and tracking, weapons guidance and delivery, and jamming of threat emitters and receivers.

The antennas used by these systems must meet specific requirements. Size, weight, reliability and maintainability are important factors that must be considered when selecting an antenna for a particular application. Size and weight restrict the locations where the antenna can be installed. Poor antenna placement can degrade the flying qualities of an aircraft and impact the performance of the avionics system. Furthermore, the antenna must be reliable and capable of withstanding prolonged exposure to the environment, especially those identified for military applications. Also, the antenna must be maintainable and require minimum repair time should a failure occur.

Another characteristic of the antenna that is of considerable interest to the avionics systems designer is the directive gain pattern, also known as the radiation pattern. In the literature, this parameter is defined as the ratio of the radiation intensity in a given direction to the radiation of an isotropic source. [1] In equation form it may be stated as

$$D_g(\theta, \phi) = \frac{4\pi U(\theta, \phi)}{P_{rad}} \quad (1-1)$$

where $U(\theta, \phi)$ is the radiation intensity (watts/unit solid angle) in the direction of θ and ϕ (see Figure 1-1) and P_{rad} is the total radiated power. A dimensionless quantity, the directive gain is important to the systems designer for two reasons:

- 1) It determines how the antenna affects the performance of the radar or communication system. The free-space directive gain pattern could be dramatically affected as a result of the antenna installation.

2) The directivity is the maximum value of D_g . It can be used to estimate the operational performance of a particular system by considering the appropriate radar range or communications equation. [2]

The antenna selected for use in an avionics system will likely be chosen because of its radiation pattern (directive gain). For example, a UHF/VHF radio system will require an antenna that can radiate in all directions to facilitate communications with other aircraft and traffic control located on the ground. The radiation pattern for such an antenna might appear as shown in Figure 1-1. This pattern is omnidirectional in azimuth.

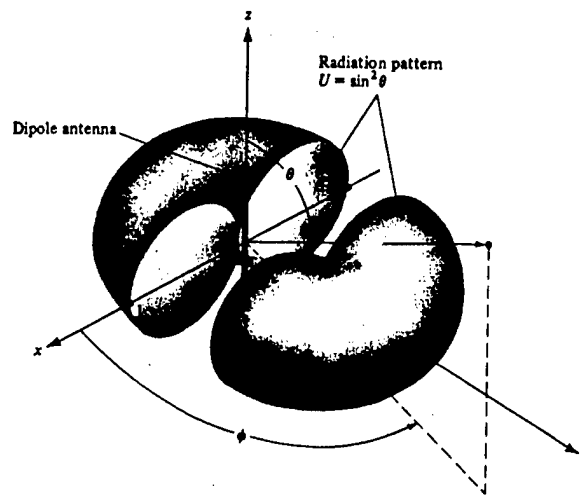


Figure 1-1: Typical radiation pattern for a communications system. From Ref. [1].

For a radar altimeter system, the antenna selected may likely be chosen for its narrow beamwidth and low sidelobes. It is necessary to have as little energy as possible radiate into undesirable directions to avoid detection. A radiation pattern of this type might appear as shown in Figure 1-2. The directive gain of this antenna tends to concentrate the radiated energy in a direction straight down, perpendicular to the flight path and minimize any energy radiated in other directions.

An antenna used for an EW system might have a radiation pattern similar to the radar altimeter system, but it is chosen for a different reason. This form of radiation pattern maximizes the power transmitted in the direction of a threat emitter or receiver, thereby maximizing the effective range of the EW system.

The avionics systems designer, having identified the antenna suited for a particular application, must determine a location on the aircraft for the antenna installation. This task is not

straightforward. Locations on the aircraft that offer the greatest field-of-view (and these areas are few) will be utilized by systems considered to be of more importance to the mission of the aircraft. The remaining areas must be utilized by the systems that are of lower priority to the operation of the aircraft.

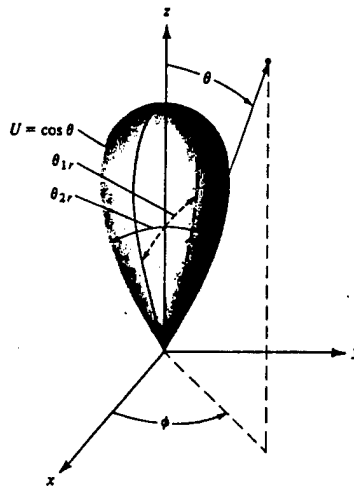


Figure 1-2: Typical radiation pattern of a radar altimeter or EW system From Ref. [1].

Some locations on the aircraft exterior that are ideal for antenna mounting, from a field-of-view perspective, may be difficult to access from within the aircraft or are environmentally harsh. An example of this is the engine bay. On the aircraft exterior, there are large areas surrounding the engine bay that are generally free of any equipment. However, underneath the aircraft skin panels, there is little or no clearance for routing of cables and connectors, let alone hardware required to secure the antenna. Furthermore, these areas must endure high temperatures and vibrations. Any equipment installed in these areas would require additional inspections and maintenance. The landing gear doors are also examples of areas that appear attractive on the surface for an antenna installation. These areas, however, are avoided because of the limited clearance allowed by the retractable landing gear, as well as the safety hazard introduced by the antenna installation. Any loose hardware or cabling could interfere with the normal operation of the landing gear jeopardizing the safety of aircrew and aircraft.

Aside from the structural and environmental issues that need to be considered when identifying a location for an antenna installation, the question of electromagnetic compatibility must be addressed. A given avionics system must operate in the vicinity of other electronic systems. Coupling between systems through radiated and conducted emissions is alleviated by

proper shielding and isolation. Therefore, it may be necessary to separate the antennas of systems operating in the same frequency band to eliminate or reduce the possibility of electromagnetic interference (EMI).

It is apparent that the task of finding a suitable location to mount an antenna is difficult, especially with several avionics systems competing for limited surface area. Nevertheless, once the location has been established, an analysis must be performed to evaluate the effective radiation pattern of the antenna when installed on the aircraft. The need for such an analysis arises from the interference that the aircraft presents to the radiating or receiving antenna. Components of the aircraft such as the fuselage, wings, engine nacelles, horizontal and vertical stabilizers, and external fuel tanks and weapons stores can dramatically affect the antenna radiation pattern.

An analysis of this nature is crucial not only during the initial design of an aircraft, but whenever a modification of a new or existing avionics system is considered which involves a change or addition of an antenna installation. Throughout the service life of a typical aircraft (many have service times of 20 years or more), it will undergo a variety of modifications and development activities. These upgrades, whether pertaining to military or general aviation, are generally implemented to improve the survivability of the aircraft in some way. Some of these modification activities will require the addition of one or more antennas. An analysis of the effective radiation pattern will help determine if the modification will perform as desired.

Knowledge of the installed radiation pattern is of further benefit to pilots and mission planners during the preparation of a mission. For example, an aircraft configured with an EW pod and external stores may have difficulty transmitting or receiving from a particular direction due to interference from the externally loaded weapons, pylons, or fuel tanks. An awareness of the true radiation pattern provides insight into determining the best route to ingress or egress a given threat area, thus maximizing the overall effectiveness of the mission.

B. DETERMINING THE RADIATION PATTERN

The avionics system designer must determine the radiation pattern of the antenna installed on the aircraft or at least attempt to make an educated estimate. One way the radiation pattern can be extracted is to develop a flight test program of the actual aircraft with the installed avionics system fully operational. The aircraft is piloted through a series of maneuvers while a ground station takes amplitude measurements of signals it receives from the airborne system. This scenario also requires that the aircraft be instrumented with sensors to provide the aircraft

attitude (roll, pitch, yaw, and heading) with respect to a reference time that is common to the aircraft and the ground station. After the flight has been completed, the aircraft attitude data is synchronized with the received signal strength measurements to develop the effective radiation pattern of the avionics system antenna. This approach, however, is very costly to implement and there exist several issues that must be considered. The first of these is the multipath propagation effect between the aircraft and the ground station. As the aircraft flies a radial path from the ground station, there will be a series of peaks and nulls in the received signal strength, the behavior of which must be quantified. Additionally, the $1/r^2$ relationship of the received signal strength must also be accounted for and factored into the measurements. Finally, it is inherently difficult if not impossible to establish certain aircraft attitudes relative to the ground station so that accurate measurements can be made. This greatly limits the breadth of information concerning the radiation patterns that can be generated from this approach.

The USAF has implemented an alternative approach at Rome Air Development Center (RADC). This facility uses salvaged airframes to evaluate their effects on radiation patterns and EW systems performance. The full-scale aircraft is mounted on pedestals that may be positioned over a wide range of attitudes and illuminated by an RF field. Static measurements are made to determine the actual radiation pattern of the antenna. This method is much more affordable than the flight test program because measurements can be made much more quickly and easily in this "laboratory" environment. When the type aircraft is available at the facility, test results can be provided in an adequate amount of time. More time and planning are required, however, if the aircraft is not included in the RADC inventory. [3] If the use of a full-scale aircraft is not convenient, then a scale model can be employed and a similar procedure executed, after an appropriate scaling in frequency, to obtain the desired data. [4]

Still another approach to the question of the effective radiation pattern for an installed antenna involves the use of numerical techniques derived from electromagnetic theory on radiation and scattering. With the advent of fast and powerful computer systems, solutions to this problem can be acquired quickly and cost effectively. Popular codes such as NEC, PATCH, and APATCH have been created to address this type of problem. NEC and PATCH solve the integral equation, the fundamental mathematical definition of this problem, by employing the method of moments. APATCH makes use of the physical optics approximation and geometrical optics. These programs require a computer model of the aircraft in a format that is compatible with the particular code being used. NEC, for example, requires that the aircraft model be comprised of

electrically short wires while PATCH and APATCH dictate that the model be created from small triangular surfaces referred to as *facets*.

The numerical approach has the advantage of being not only cost effective and expedient, but accurate as well, when compared with measured data. Furthermore, the problem can be analyzed well in advance of the manufacture of any models or full-scale prototypes. Various locations for antenna installations can be compared based on the numerically derived results. The avionics systems designer can then choose an optimum location while considering other important factors such as accessibility, maintainability, and sufficient EMI isolation when needed.

C. THESIS OUTLINE

Chapter II presents a cursory review of the methods available to solve this type of problem and concludes with a justification for the use of APATCH. The measured radiation pattern for a telemetry antenna is compared to that derived from APATCH as well as the pattern predicted by another electromagnetic computer code.

Chapter III contains a discussion of the installed antenna patterns for several aircraft/antenna systems that were analyzed. The first is the C-172 aircraft with a quarter-wavelength monopole. This combination is proposed for the Traffic Alert and Collision Avoidance System (TCAS) that is being considered by the Federal Aviation Administration for general aviation aircraft. A second case that was investigated is an F-18 aircraft with a telemetry antenna. This type of antenna is found primarily in the flight test community and is part of the instrumentation system that transmits data to test mission control activities located on the ground. Chapter IV contains a summary and final remarks.

II. OVERVIEW OF ELECTROMAGNETIC CONCEPTS

In this chapter, some concepts in electromagnetics that are relevant to the problem under consideration are discussed. A brief presentation of APATCH, the program used to compute the radiation pattern of an installed antenna, is also provided. The chapter concludes with a comparison of APATCH results and measured data for the case of a cylinder with a telemetry antenna. Also included are the results from PATCH, an electromagnetic code based on the method of moments.

A. SCATTERING MECHANISMS

When an antenna is allowed to radiate in free-space, its radiation pattern can be predicted quite easily. However, if a scatterer, such as an aircraft, is located within the vicinity of the radiating antenna, then an interaction between the two arises. The nature of this interaction takes on a variety of forms, and the resulting shape of the radiation pattern is altered.

In general, when a scatterer is immersed in an electromagnetic field, two phenomena that dictate the behavior of the resulting interaction can be identified. They are absorption and scattering. Absorption occurs when some part of the impinging electromagnetic energy penetrates the surface of a material. The amount of absorption that takes place depends on the electrical properties of the material, i.e., the permittivity (ϵ), permeability (μ), and conductivity (σ). A thorough discussion of this type of electromagnetic action is found in [5].

The second class of interaction that one observes between an impinging electromagnetic field and a structure is known as scattering. This phenomenon results in the re-radiation of energy into the medium containing the impinging electromagnetic field. Here, as well, the amount of scattering depends on the electrical properties of the scatterer. An additional factor affecting the scattered electromagnetic field is the shape of the scatterer. The scattering from the platform is a complex function of observation angle and frequency. However, it is usually possible to associate features in the scattering pattern with distinct physical mechanisms. Figure 2-1 depicts several of these scattering mechanisms. Three categories of scattering can be identified in this figure: surface waves, diffraction, and specular reflection.

Surface waves radiate as they propagate along two or three-dimensional discontinuities on a scatterer. Discontinuities include both electrical and physical boundaries between materials.

When these surface waves encounter a termination of the surface, a reflection may occur. The reflected surface wave is a source of additional radiation as it propagates along the exterior of the scatterer.

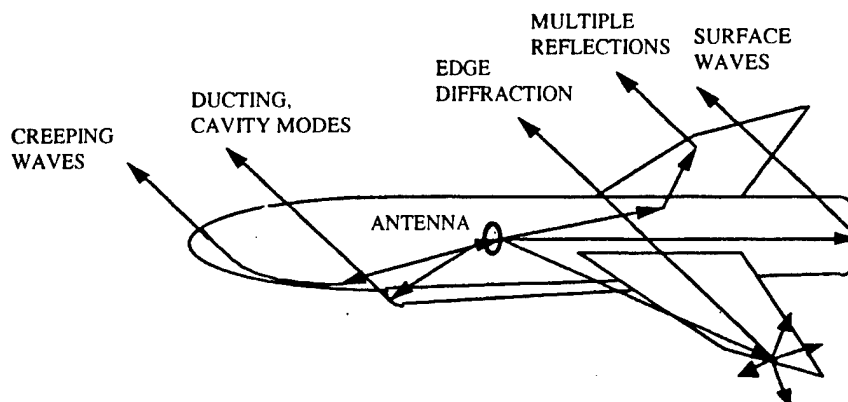


Figure 2-1: Scattering mechanisms due to interaction between an antenna and the platform. From Ref. [6].

Alternatively, upon encountering the edge, the surface wave could radiate its energy from this point or edge producing a diffracted field. The leading and trailing edges of aircraft wings are examples of surface discontinuities where diffraction can occur.

The final scattering mechanism to consider is called specular reflection. Snell's law predicts this type of phenomenon. Multiple reflections arise when the incident field reflects from two or more surfaces located on the scatterer. [4] The reflected fields arriving at a point in the field far from the scatterer can combine in a manner producing constructive or destructive interference. Specular reflection is the dominant scattering mechanism when the physical dimensions of the scatterer are much larger than the wavelength and the observation direction satisfies Snell's law.

B. SURVEY OF METHODS USED TO SOLVE THE SCATTERING PROBLEM

With regard to the problem at hand, that is, the prediction of the antenna's radiation pattern when installed on an aircraft, a variety of techniques is available for obtaining a solution. Geometrical optics (GO), physical optics (PO), integral equations, and diffraction theory are among the more familiar methods used to analyze this type of problem. Due to the nature of the problem, it may be more desirable to use one method over another. [7] Furthermore, it has been suggested that a hybridization approach be implemented, which is a combination of two or more

methods that capitalize on the desirable features of each technique. [8] The following is a brief discussion of the advantages and disadvantages of the various methods.

The first method to consider, known as Geometrical Optics (GO), is a high frequency technique used to determine the fields reflected from a scatterer. While it was originally developed to aid in the study of the propagation of light, GO can be used here as well to solve this problem. The GO approach analyzes rays that are coincident with the direction of propagation of the incident field. Snell's Law (the angle of reflection equals the angle of incidence) is used to predict the direction of the reflected rays. The reflected field, $\vec{E}_r(s)$, at an observation point located the distance s from the point of reflection Q_r that lies on the surface of the scatterer is

$$\vec{E}_r(s) = \underbrace{\vec{E}_i(Q_r)}_{\text{Field at reference point } (Q_r)} \cdot \underbrace{\bar{R}}_{\text{Coefficient of reflection}} \cdot \underbrace{\sqrt{\frac{\rho_1' \rho_2'}{(\rho_1' + s)(\rho_2' + s)}}}_{\text{Spatial attenuation and spreading factor}} \underbrace{e^{-j\beta s}}_{\text{Phase factor}} \quad (2-1)$$

where \vec{E}_i is the incident field at the reflection point Q_r , and the reflection coefficient, \bar{R} , is determined by the constitutive parameters of the reflecting surface. To account for the spreading of the reflected field as it propagates along the path length s , a spatial attenuation and spreading factor is included in the expression. This parameter depends not only on the path length, but also on the radii of curvature of the reflected wavefronts given by ρ_1' and ρ_2' . The phase of the reflected field is determined by the phase constant β .

For sufficiently high frequency, the scattered field may largely be predicted by GO. However, this technique fails to predict the portion of the scattered field resulting from diffraction occurring at an edge, vertex, or corner. Furthermore, GO predicts zero fields in the shadow regions. [7] The Geometrical Theory of Diffraction (GTD) is a technique used to determine this part of the total scattered field. It requires that a matrix of diffraction coefficients be determined for a given geometry. The diffracted field will be linearly related to the incident field by these diffraction coefficients. [4]

The next technique to be considered involves an integral equation. This method requires that the current density induced on the surface of a scatterer by the incident electromagnetic field be determined. The integral equation is expressed in terms of the unknown current density. It is solved by approximating the current density with a finite series of basis functions of unknown complex coefficients. This leads to a reduction of the integral equation into a system of algebraic equations that can be solved by an application of matrix manipulations. The well-known

numerical procedure to solve the integral equation is the method of moments. [7] Once the current density has been found, the scattered field is computed from the radiation integrals.

Physical optics (PO) is another high frequency method. Unlike GO which tracks the paths of rays, PO is current based. In this method, a scatterer is replaced with an imaginary surface over which the geometrical optics current flows. When the scatterer is electrically large, the current density \vec{J}_p may be approximated by

$$\vec{J}_p \approx 2\hat{n} \times \vec{H}_i \quad (2-2)$$

where \vec{H}_i is the incident magnetic field on the surface of the scatterer, and \hat{n} is a unit vector normal to the surface. Having established the current density, the evaluation of the scattered field is straightforward. As a result of the PO approximation, this technique has direct applicability to the problem at hand. Generally, it is the case that the dimensions of the scatterer (i.e., the aircraft components) are many times the operating wavelength. [7]

Like the GTD, the Physical Theory of Diffraction (PTD) is an edge diffraction model. It is a complement to the PO method. The PTD approach, however, is different than the GTD in that the diffracted field is determined by an estimate of a fringe current, a current flowing along the surface discontinuity. The fringe current is found from the analysis of a corresponding canonical scattering problem. [4]

Of the methods described, the solution provided by the integral equation is most accurate in that no approximations are made in the formulation of the problem. The method of moments, which is the corresponding numerical algorithm to solve the integral equation, is used extensively. Computer codes are available that have implemented the moment method, NEC and PATCH, for example. These codes lend themselves to a wide array of problems from simple geometries to more complicated ones involving large scatterers. However, as the dimensions of the scatterer increase compared to the wavelength, so does the corresponding matrix resulting from the moment method. Therefore, the computation times increase rapidly in proportion to the physical size of the scatterer.

When the physical dimensions of the scatterer are sufficiently large compared to the wavelength, generally ten wavelengths or more, the high frequency techniques can be applied to solve the problem. A hybrid technique called Shooting and Bouncing Rays (SBR) utilizes PO and GO in a systematic way to characterize the scattering behavior from large bodies. [9] APATCH is a computer code that makes use of SBR to compute the radiation patterns from antennas situated on large scattering platforms.

Figure 2-2 illustrates the SBR technique. The SBR concept is applied to an example consisting of a point source, a curved surface, a plate (which serves as a secondary reflector), and two observation points. First, neglecting the presence of the scatterers (the curved surface and the plate), rays are launched from the point source, and the incident field is determined over all observation angles. Next, areas on the curved surface that are directly illuminated by the source are locations where a scattered field is computed using the PO approximation. Rays from the scattered field can then be used to determine the total field (at observation point #1, for example) or tracked onto secondary scatterers such as the plate using GO. The field at observation point #2 is determined by a superposition of the incident ray and the scattered ray that was derived from PO. Additional contributions to the field at this location come from rays arriving from secondary reflections that have been tracked by GO or from scattered field components computed by an additional application of PO. [8]

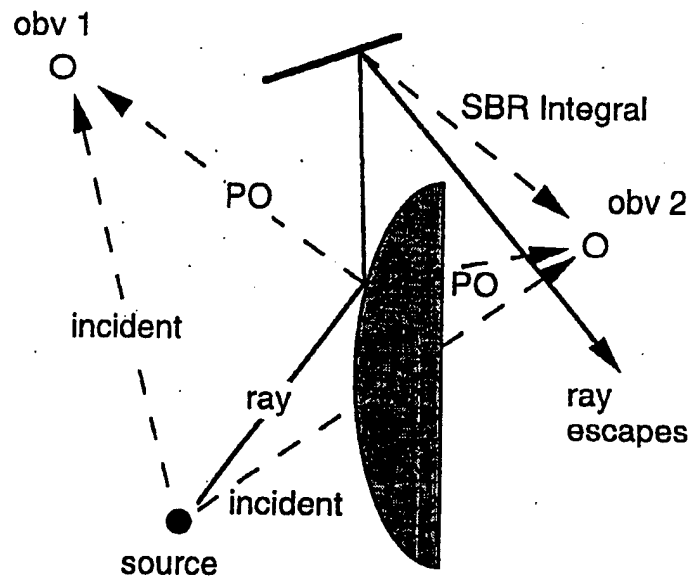


Figure 2-2: Geometry of Shooting and Bouncing Rays. From Ref. [8].

References [8], [10], and [11] established the validity of SBR by analyzing some fundamental shapes such as the trihedral and the cylindrical cavity. These papers showed that as the shapes decreased in size, the dominance of specular reflection begins to subside and the effect of other scattering mechanisms, such as edge diffraction and surface waves, becomes more

apparent. It should be stated that these papers addressed the subject of the RCS of the fundamental shapes. Nevertheless, the same scattering mechanisms that govern the behavior of the RCS are also relevant to the analysis of the radiation patterns for antennas installed on large scattering platforms. Thus, the SBR concept can be extended to the problem under consideration.

C. APATCH

APATCH has been created to model the effective radiation pattern of antennas in the vicinity of electrically large scattering objects. Developed by DEMACO Inc, it is written in Fortran and C programming languages. It employs PO, GO, and diffraction theory iteratively over many observation angles to arrive at the desired results. The program output is a data file containing observation angles versus directivity.

The following is a brief description of the use of APATCH and associated software programs. Figure 2-3 shows how various programs and files are used collectively. Beginning with the ACAD program, a model of the aircraft must be created if it does not already exist. ACAD (Advanced Computer Aided Design) was developed by Lockheed-Martin beginning in 1982. It is written mostly in PASCAL with supplementary code written in C. The benefit of ACAD is its ability to generate files that can be interfaced with other utilities that specialize in an area of analysis such as RCS or computational fluid dynamics. This program has also been adopted by the DoD Electromagnetic Consortium. [12] The program creates the aircraft model in the facet file format, which is compatible with APATCH. The model is made up of small triangular facets. Each facet is a location where APATCH applies the PO approximation and GO.

APATCH requires that all the necessary information concerning a given problem be contained in an input file. It is identified in the working directory by the filename extension *.ap_input. Within this file is information such as the filename of the aircraft ACAD model, specific parameters about the antenna under consideration, operating frequency, and the observation angles of interest. To execute the program, at the system prompt, the user enters:

apatch filename

A library of antenna classes (sources) is available in APATCH. Included among the sources are the dipole, monopole, and rectangular or circular waveguide. One of them must be included in the APATCH input file. If desired, an array of sources can be constructed to give a specified free-space radiation pattern and then incorporated into the input file to establish the true pattern in the presence of the scatterer. One source class that is flexible and capable of simulating a variety of antennas is the current source. By combining them in a systematic way, a wide

variety of free-space antenna patterns can be represented. Also, if required, by using an equivalent set of these current sources, a complex current distribution can be represented. [13]

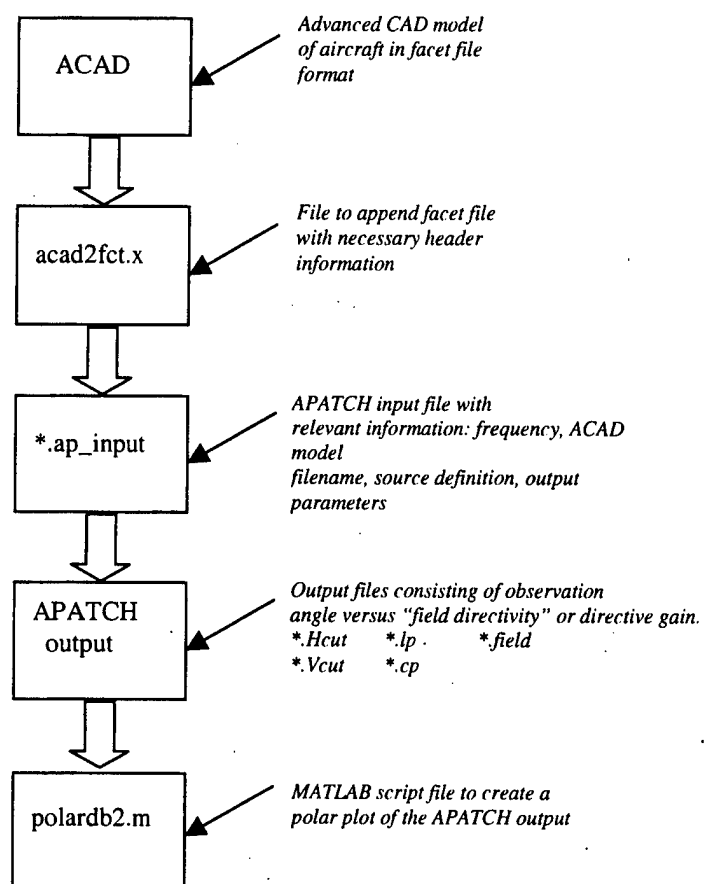


Figure 2-3: Various programs used collectively. Asterisk (*) denotes an arbitrary filename.

The output is determined from the geometry, source, and computation specifications defined within the input file. Generally, a set of sector cuts is desired which provides a listing of reference (observation) angles versus the electric field strength or directive gain. Figure 2-4 defines the orientation of the E_θ and E_ϕ polarizations that are the output of the typical APATCH run. Both polarizations are tangent to the observation sphere. While the size of the sphere is not specified in the APATCH program, it is assumed to be equivalent to the far-field distance where the electric field has a $1/r$ dependence and the non-propagating field components ($1/r^2$, $1/r^3$) have diminished. [13]

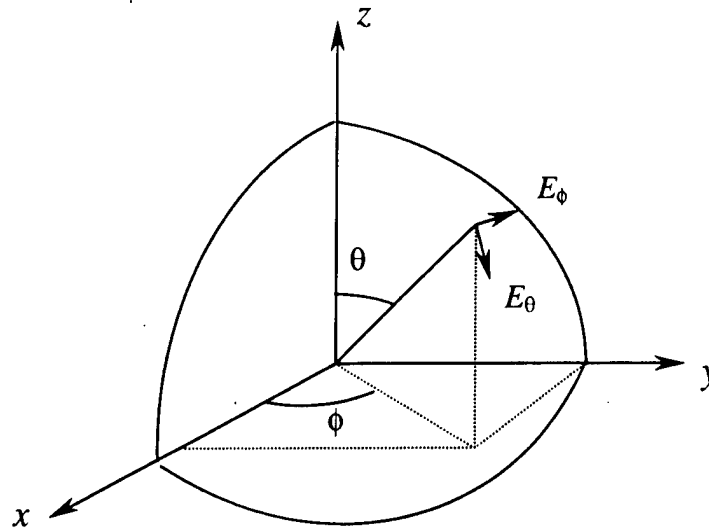


Figure 2-4: Coordinate system showing orthogonal electric field vectors

D. PRELIMINARY STUDY

To evaluate the performance of APATCH and to lay the foundation for study of other scattering geometries, a test case was run for a telemetry antenna located on a cylinder, for which measured data was available. Telemetry antennas are found throughout the flight test community and are installed on all types of test aircraft. They are used with the flight test instrumentation system to acquire and transmit data to a ground station that is monitoring certain parameters that are relevant to the test mission. Its construction is a quarter-wavelength wire that is excited from one end. The wire is inclined at a 45° angle with respect to the vertical, and the assembly is encased in an aerodynamically shaped material that is electrically transparent (see Figure 2-5).

Haigh-Farr and TECOM are two manufacturers of this type of antenna. Measurement data of the antenna mounted on an 8-inch diameter by 30-inch length cylinder was available from Haigh-Farr. This data was used to compare with the results derived from APATCH. The cylinder model referenced in the APATCH input file is shown in Figure 2-6. While not included in the ACAD model, the input file contains the location of the telemetry antenna with respect to the cylinder coordinates. It is situated halfway along the length of the cylinder.

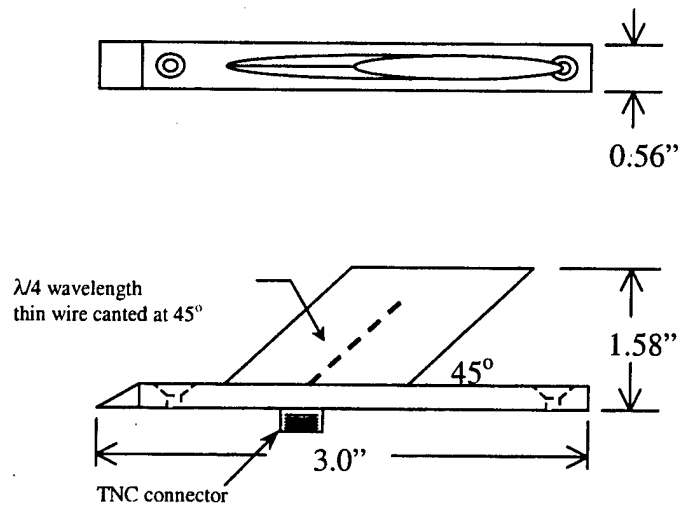


Figure 2-5: Telemetry antenna, frequency 2.25 GHz

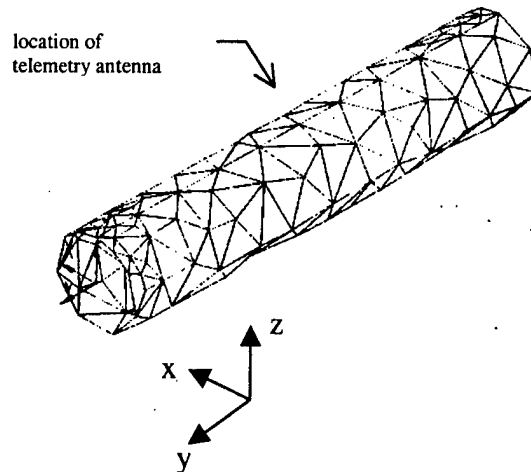


Figure 2-6: ACAD model of cylinder.

A comparison of APATCH results with the measured data is made in Figure 2-7. Each curve on the plots was normalized to its maximum value with the exception of those in Figure 2-7b to facilitate comparison. The y-z plot (or elevation plane) is computed by APATCH by setting the reference angle ϕ to a constant value and varying θ in the y-z plane (reference Figure 2-4). Similarly, the x-y plot (or azimuth plane) is determined by setting θ constant and varying ϕ in the x-y plane. To convert the spherical angles θ and ϕ into the familiar azimuth and elevation angles, the following relationships are used:

$$\text{Azimuth} = -\phi \quad (2-3a)$$

$$\text{Elevation} = \theta - 90^\circ \quad (2-3b)$$

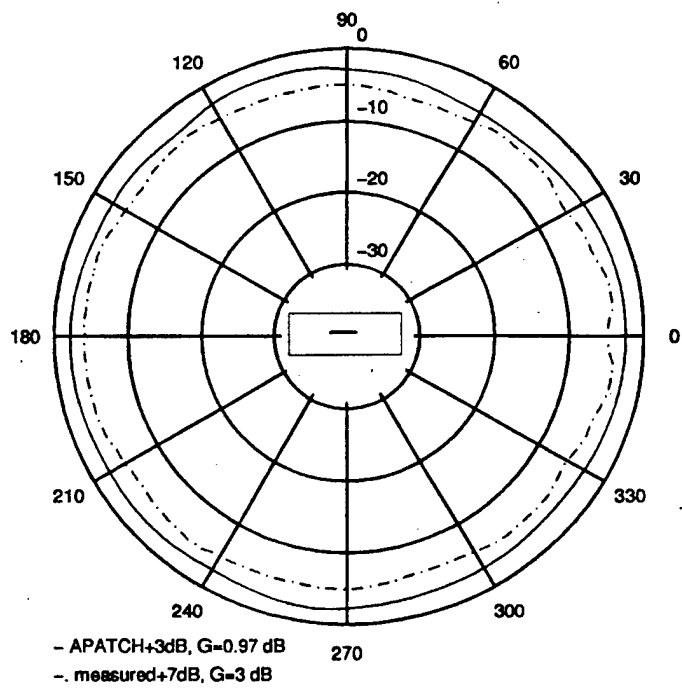
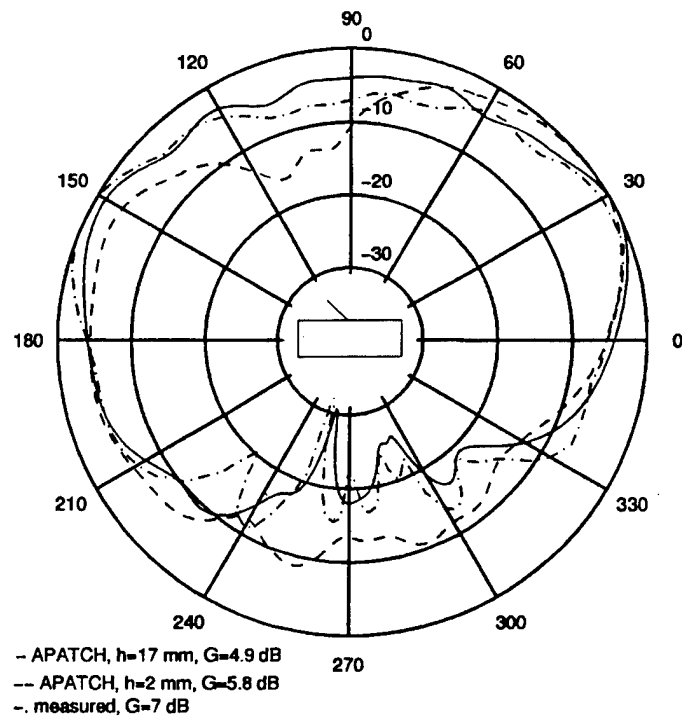


Figure 2-7: APATCH results compared with measured data for cylinder and telemetry antenna. (a) y-z (elevation) plane, (b) x-y (azimuth) plane

Referring to Figure 2-7a, the y-z plane pattern, APATCH (shown in the solid line) approximates the behavior of the measured data. On the upper part of the plot ($0^\circ < \theta < 180^\circ$), most of the APATCH result is very acceptable. The largest disparity in this part of the curve is approximately 3 dB at $\theta = 90^\circ$. Considering the region below the cylinder ($180^\circ < \theta < 360^\circ$), APATCH exhibits difficulty predicting some of the peaks and nulls in the measured data because the calculation did not include edge diffraction or radiation from surface waves in its solution. At $\theta \cong 230^\circ$, where the measured data shows a dip in the pattern, there is at least a 10 dB difference between the empirical data and the calculated results.

The telemetry antenna was modeled as a current source. This is one of the built-in antenna classes available in the APATCH program. It is a point source that launches rays with a dipole weighting. [13] Since this antenna class makes no provisions for the control of the length and radius of the radiating element, the height of the current source was varied until a good agreement between the computed results and the measured data was achieved. In this way, a means is provided of compensating for the effect of the length and radius of the actual radiating element. Figure 2-7a includes the initial result when the height of the current source above the cylinder was set to 2 mm. The best match to the measured data was found to be when the height equaled 17 mm, which corresponds to a distance of $\lambda/8$.

The x-y plane pattern computed by APATCH closely resembles the measured data as shown in Figure 2-7b. Both curves have been shifted from their normalized value for clarity. The symmetric behavior of the scattered field about the scatterer is exhibited in these plots.

The effect of surface waves and edge diffraction should be accounted for whenever possible in a numerical solution because these scattering phenomena contribute significantly to the total field in directions away from the pattern maximum, as can be seen in the region below the cylinder. APATCH does not compute the portion of the scattered field due to surface wave propagation since it is based on the PO approximation and GO. These high frequency methods are accurate in accounting for the field due to specular reflection, but not surface waves or edge diffraction. A feature within APATCH allows for the computation of the field due to edge diffraction. It requires the creation of an "edge file," which is a sequential list containing edge length, orientation, and wedge angle for all edges contained in the ACAD model. While this utility was implemented, it did not enhance the pattern in the region below the cylinder. In fact, some discontinuities were introduced into the radiation pattern where the diffracted field is blocked by the surface.

The APATCH results applied to the problem of the cylinder with the telemetry antenna are generally in good agreement with the measured data. Surface wave propagation (creeping waves) is the predominant scattering mechanism in the region below the cylinder and explains why APATCH can not reproduce all of the sharp peaks and nulls observed in the measured data. This region is referred to as the shadow region, the area where GO does not predict any field components. Additionally, the open ends of the cylinder are sources of double edge diffraction, which was not considered in the APATCH solution.

E. PATCH

PATCH, an electromagnetic code based on the method of moments, was used to investigate the cylinder with the telemetry antenna. Unlike APATCH, which specifies that the scattering geometry be modeled without the antenna, PATCH requires that the cylinder and antenna be modeled together. Figure 2-8 shows a detail of the region where the cylinder and antenna come together in the ACAD model. One of the edges of the facets comprising the antenna is excited, and PATCH computes the resulting scattered field from this geometry.

Figure 2-9 shows the elevation plane pattern. Immediately, it is apparent that PATCH calculates the interaction between the cylinder and the antenna quite accurately. Even the sharp peaks and nulls in the radiation pattern below the cylinder are included in the PATCH results. The program computed the gain to be 4.1 dB (compared with 4.9 dB from APATCH). Because PATCH is a method-of-moments code, from a practical perspective, it cannot be used to compute the radiation patterns of antennas on electrically large aircraft. Computation times for problems involving large scattering geometries (10λ or more) can be quite high. Furthermore, the demand for computer memory rises very quickly as the electrical size of the scattering geometry increases.

The SBR approach implemented in APATCH showed good results in computing the radiation pattern of the cylinder with the telemetry antenna. The reasons for any discrepancies in its performance were explained. A comparison between the PATCH and APATCH results can be made indicating that there is little advantage to the use of a moment-method code in this particular problem. In the next chapter, the radiation patterns for antennas situated on aircraft are presented. The size of the aircraft that were considered are all greater than 10λ , so the use of APATCH in the succeeding analysis is required.

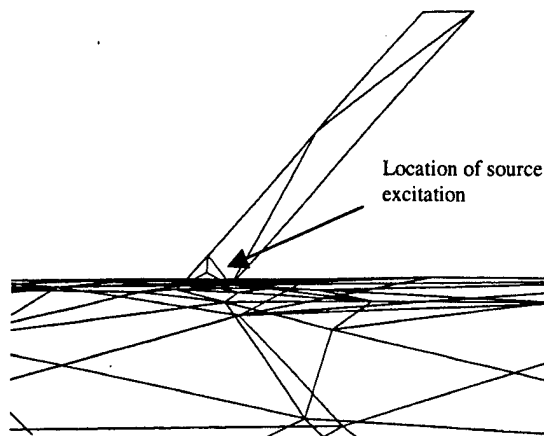


Figure 2-8: Detail of ACAD model used in PATCH code. Figure indicates the location of the source excitation.

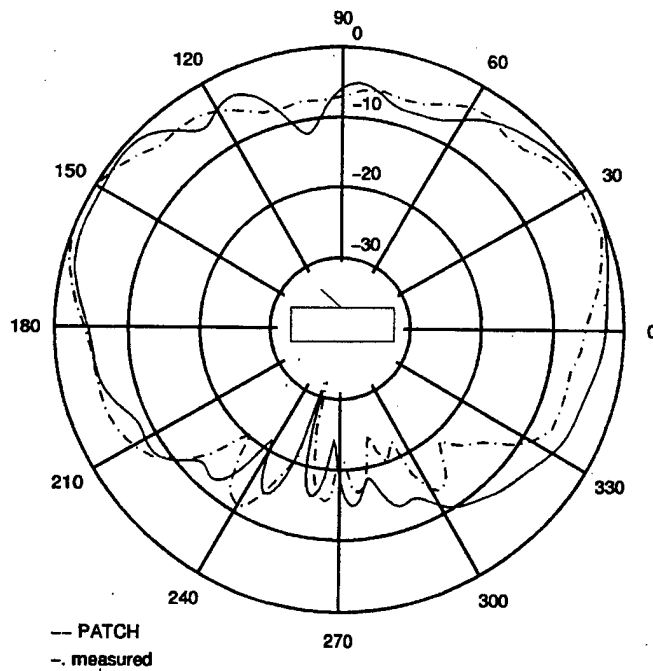


Figure 2-9: PATCH results for cylinder with telemetry antenna. Elevation plane shown.

III. AIRCRAFT/ANTENNA SYSTEM EVALUATIONS

Having established that the high frequency methods presented in Chapter II are suitable to analyze the problem under consideration, several aircraft/antenna systems are examined. APATCH was used to compute the scattered field resulting from the interaction between the aircraft and the installed antenna. For each aircraft, an antenna associated with a common avionics function was placed at various locations and its performance ascertained from APATCH. The results are presented as before, that is, in the form of polar plots that have been normalized to the maximum value for each curve. All plots are referenced to the aircraft planes of rotation: roll, pitch and yaw.

A. CESSNA 172 WITH TCAS ANTENNA

The first problem involved the Cessna 172 (C-172) aircraft. An antenna suitable for use with the Traffic Alert and Collision Avoidance System (TCAS) is analyzed. The use of TCAS is mandated by the FAA for use on all passenger and cargo aircraft with 10 seats or more. It is used by pilots to determine the presence of nearby aircraft. TCAS operates by interrogating the transponder of an approaching aircraft. Range is determined from the time required to receive the reply, and altitude is extracted from the information encoded within the reply. Mode C is the term used to describe a transponder that reports its altitude when interrogated. In a complete TCAS system, the bearing to the approaching aircraft is determined by a pair of directional antennas. This version is not explored here. Instead, only an omni-directional antenna is considered, which only yields the range and altitude of an intruding aircraft. It is proposed that bearing be determined from a position reporting feature of a transponder similar to Mode C operation.

The aircraft model used in the following analysis is shown in Figure 3-1. Indicated in the figure are the locations that were considered for antenna placement. A vertically polarized quarter-wavelength monopole antenna was used, which in free space produces an omni-directional radiation pattern (see Figure 1-1). TCAS operates on two frequencies. It interrogates (transmits) on 1030 MHz and receives transponder replies on 1090 MHz. Figures 3-2 through 3-4 contain the radiation patterns corresponding to both frequencies.

First, the antenna installed at location A is analyzed. Corresponding radiation patterns for the roll, pitch and yaw planes are shown in Figure 3-2. The patterns for both frequencies (interrogate and reply) have been plotted. Each plot is normalized to the maximum value and

labeled accordingly. Upon inspection of the roll plane pattern (Figure 3-2a), it appears that there is good coverage from angles just below the horizon to approximately 30° above the horizon. There is equal coverage on both the left and right sides of the aircraft in the space above the wings. This is beneficial because pilot visibility in this region is limited due to the high mounted wings on this aircraft. Underneath the aircraft, the radiation exhibits sharp peaks and nulls with the peaks being approximately 10 dB below the maximum value (5.0 dB for this plot). However, adequate coverage below the aircraft can not be expected with the antenna installed at this location.

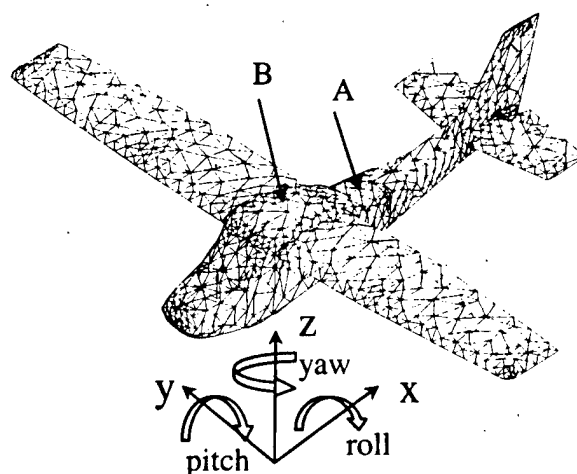
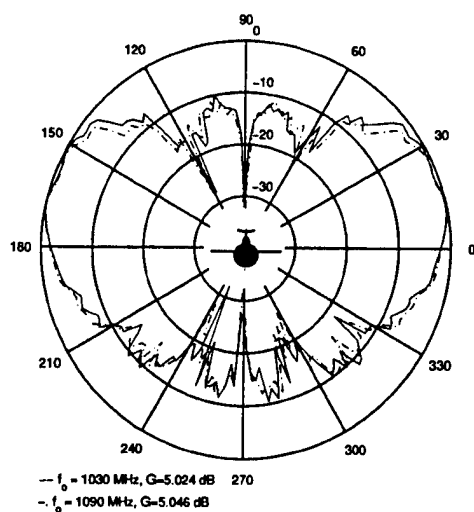


Figure 3-1: ACAD model of C-172 aircraft. Planes of rotation are roll pitch and yaw.

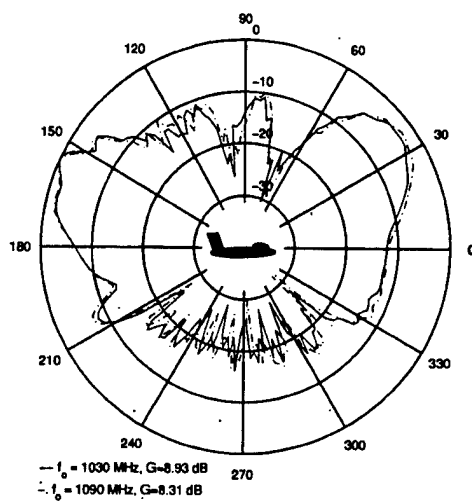
The pitch plane pattern (Figure 3-2b) shows the coverage forward and aft of the aircraft. The space forward of the aircraft does not appear to have as complete coverage as in the space behind the aircraft. In fact, the point of maximum gain is found in the aft region.

Figure 3-2c is the yaw plane pattern. There is a gain of approximately 3.7 dB in the region behind the aircraft but only -3 dB in the region in front. The decrease in the gain in the forward space is due to the placement of the antenna. Its field-of-view is blocked in the forward direction by the aft cabin window, which is modeled as a conducting surface. More complicated modeling is necessary to determine how the scattered field is affected as it propagates through the aft window and within the cabin interior. Nevertheless, it is probably safe to assume that there is negligible contribution to the scattered field in the forward direction due to any rays that have

(a)



(b)



(c)

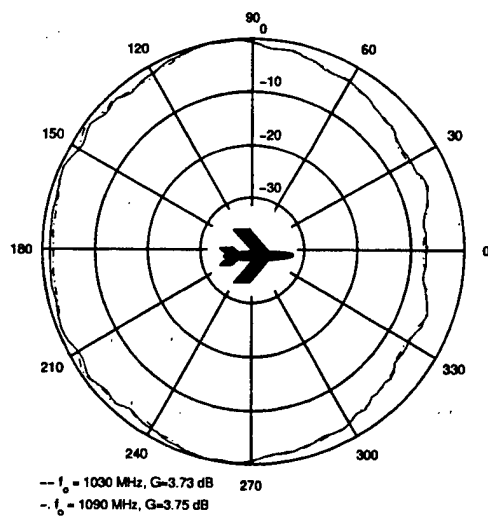


Figure 3-2: Polar plots for C-172 with TCAS antenna at location A. (a) roll, (b) pitch and (c) yaw

escaped from within the cabin interior. The dip in the gain in this direction is not a desirable feature of a TCAS antenna. It is imperative that the highest gain occur in the space in front of the aircraft, where a collision is more likely to occur. [14]

A second set of simulations was performed with the antenna mounted at location B. The results are plotted in Figure 3-3. The roll pattern, Figure 3-3a, shows that the antenna performs very well in the region above the aircraft, except for directly above, where there exists a sharp null in the pattern. This is typical, however, of vertically polarized antennas. Comparing this figure with the corresponding plot from location A, it can be seen that there is less coverage in the region from the horizon to approximately 30° below the horizon. This is the effect of the wings on the pattern since the antenna is masked by the large wing surfaces. It should be noted, however, that the gain is about 8 dB, which is approximately 3 dB higher than when the antenna is installed at location A.

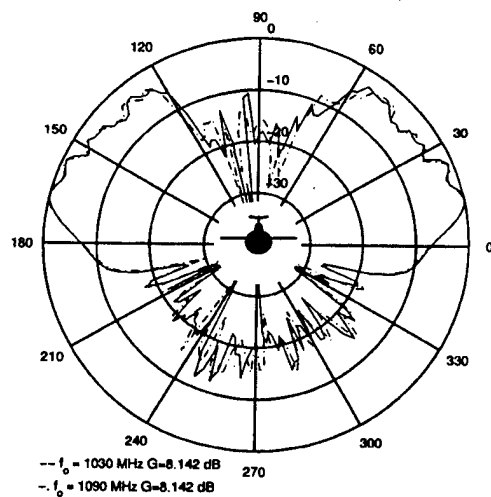
Referring to the pitch plane pattern, Figure 3-3b, the performance of the antenna in this plane is similar to that when the antenna is placed at location A. The gain in the aft region is higher than in the front.

The yaw plane pattern is shown in Fig 3-3c. It shows a more uniform pattern on the horizontal plane surrounding the aircraft. Antenna gain in the forward direction is comparable to that found in the aft region.

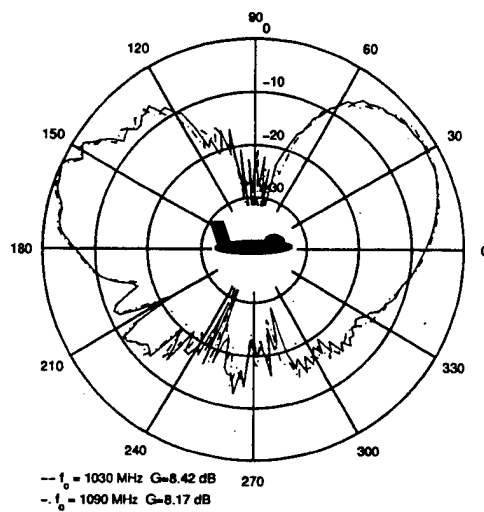
The antenna mounted at location B performs better than that at location A. The field-of-view in the horizontal plane in front of the aircraft is improved over that at location A. Furthermore, the interaction with the wings gives an increased gain that improves the detection range in this critical region where the pilot experiences obstructed visibility. If the gain in the aft region could be reduced in exchange for greater coverage in the forward region, this would improve TCAS performance and aircraft safety even more.

An antenna that could produce this effect is made up of an array of elements. A simple system can be manufactured consisting of two vertical elements, each a quarter-wavelength long. These elements are separated by one-quarter wavelength and positioned at location B, coincident with the pitch plane of the aircraft. The aft element is fed 90° out of phase with respect to the forward element. This arrangement of elements has the effect of reinforcing the field in the forward space while decreasing the gain in the aft direction. Figure 3-4 shows the free-space radiation pattern for the two-element array. These patterns have been computed by APATCH in the absence of any scattering geometry. Still another antenna architecture consists of an array of one or more passive elements and one excited element. [1] This alternative is more cost effective

(a)



(b)



(c)

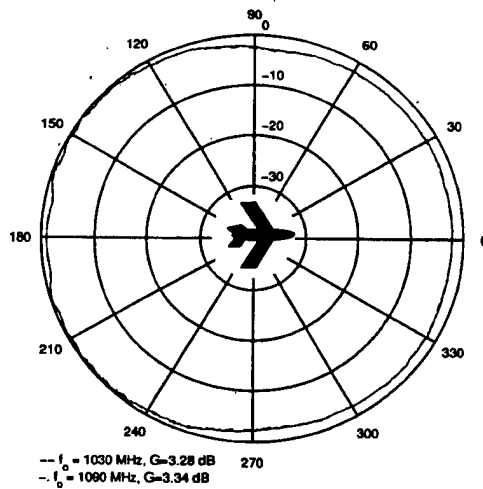


Figure 3-3: Polar plots for C-172 with TCAS antenna at location B.
(a) roll, (b) pitch and (c) yaw

and easier to manufacture, but can not be simulated directly by APATCH. The two-element array with both elements excited was modeled in APATCH, and the resulting interaction between this system of elements and the aircraft is plotted in Figure 3-5.

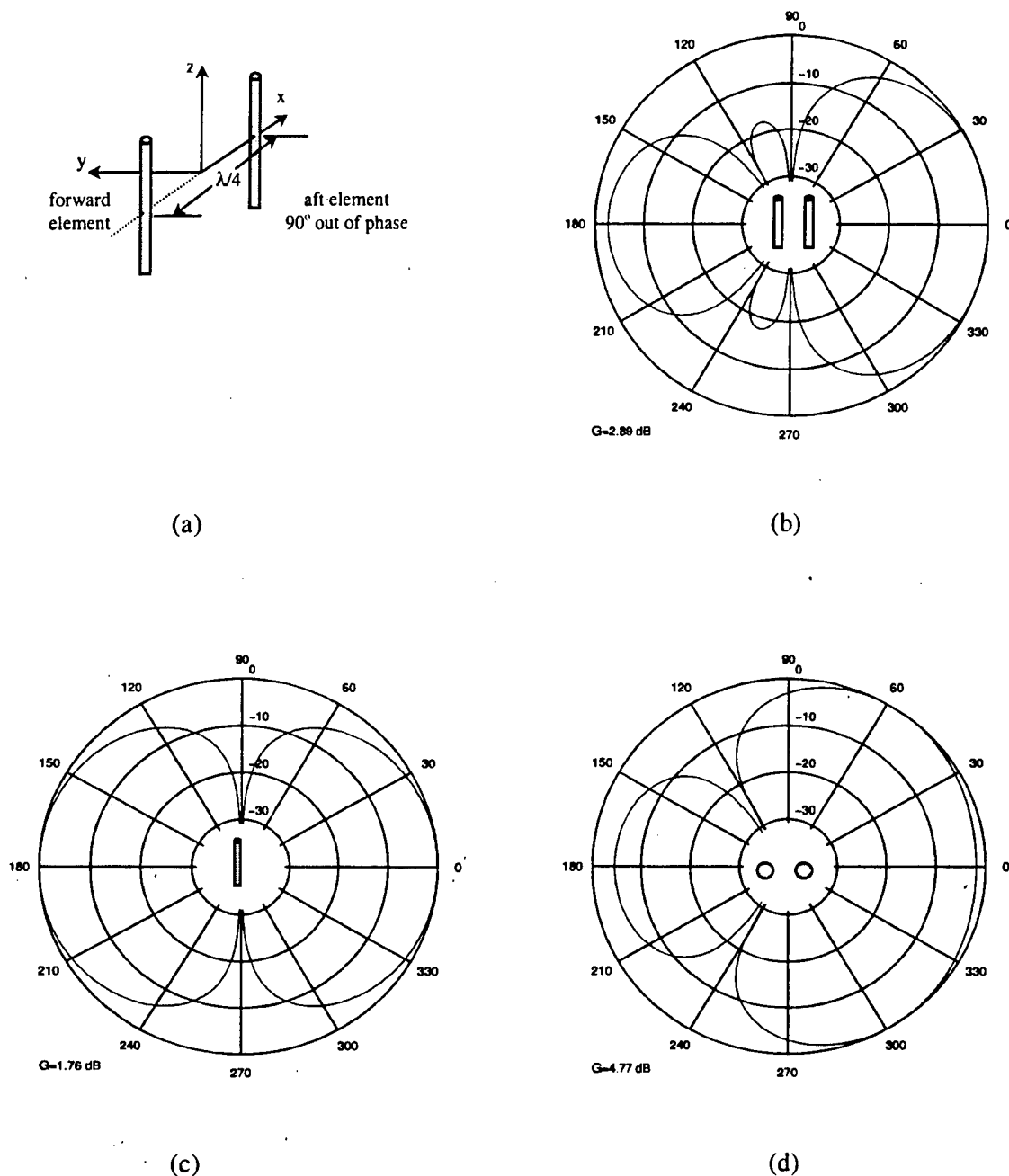
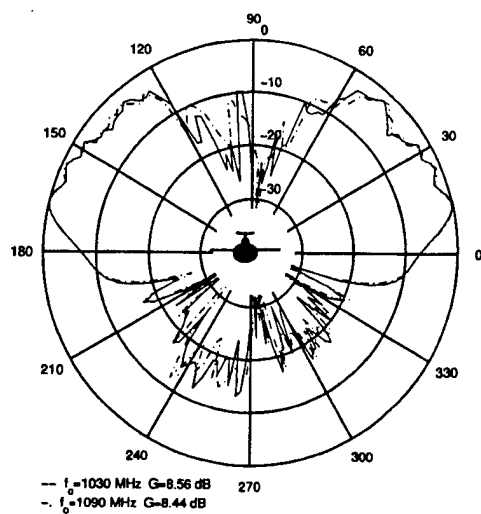
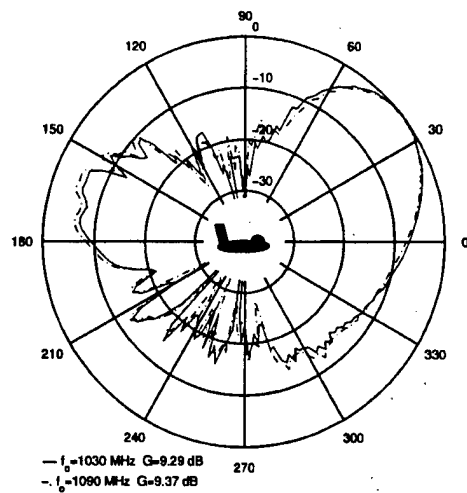


Figure 3-4: Free-space radiation pattern for two-element array. (a) arrangement of elements, (b) pitch plane, (c) roll plane, (d) yaw plane

(a)



(b)



(c)

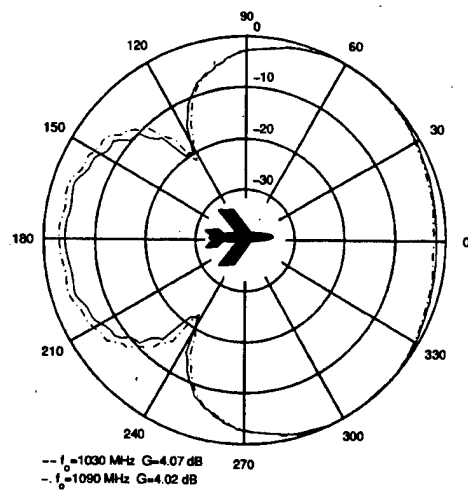


Figure 3-5: Polar plots for C-172 with TCAS two element array at location B. (a) roll, (b) pitch and (c) yaw

The roll plane pattern (Figure 3-5a) shows that the coverage in the space above the aircraft is similar to the single antenna at the same location. The gain has increased slightly from 8.14 dB to 8.56 dB for $f_0=1030$ MHz. The asymmetry observed in this plane is likely due to fact that the facet model does not possess this property.

In the plots of the pitch and yaw planes, the benefit of the array becomes apparent. Figure 3-5b shows the pitch plane pattern. The increase in gain in the forward direction is evident. Gain in this direction exceeds the gain in the aft region. Furthermore, comparing this figure with the corresponding plot for the single element, Figure 3-3b, one sees that there is a gain advantage of approximately 3 dB in the forward direction when the array system is utilized.

A similar conclusion can be made from Figure 3-5c, the yaw plane pattern. Here as well, the gain in the forward direction is greater than that in the aft direction, which improves the detection range of the TCAS system. Additionally, when compared with the single element antenna, a net gain of 0.8 dB is achieved in the horizontal plane.

From the preceding analysis, it can be concluded that location B is the better choice for the antenna installation. This location offers a greater field-of-view in the forward region where coverage is of a higher priority. Moreover, the high wing mounting of this type of aircraft restricts the pilot's visibility in the space above the wings, but the interaction between this surface and the TCAS antenna gives good coverage in this region. One point of concern is with the null that exists immediately above the aircraft. It is conceivable that an approaching aircraft could remain undetected if its flight path were one that was descending on a route parallel with the TCAS equipped C-172. The approaching aircraft could remain in this null and not be interrogated by TCAS.

While the two-element array offers advantages over the single element, such as the increase in gain in the forward direction and the space above the wings, the null occurring immediately above the aircraft still remains. The TCAS engineer must decide whether or not to pursue the design of an antenna that eliminates this null in the radiation pattern. Cost and the complexity of the antenna would have to be considered. Furthermore, the philosophy behind the development of TCAS needs to be brought into mind. The intent of TCAS is not to replace the current air traffic control (ATC) activities already in operation. Instead, the purpose of TCAS is to augment ATC capabilities and reduce their workload, thus improving the overall level of flying safety.

B. F-18 HORNET WITH TELEMETRY ANTENNA

The next configuration considered was that of the F-18 Hornet with a telemetry antenna. As described previously, a telemetry antenna is part of the instrumentation system that is installed on flight test aircraft. The instrumentation system (see Figure 3-6) gathers data from the aircraft systems under development. Generally, these systems include radar, avionics, weapons, engine, and performance and flying qualities. The data that is acquired by the instrumentation system is formatted into a PCM stream and then transmitted to a test mission control facility. From there, various parameters are monitored to assess the safety of the test and ensure that the objectives of the flight are achieved.

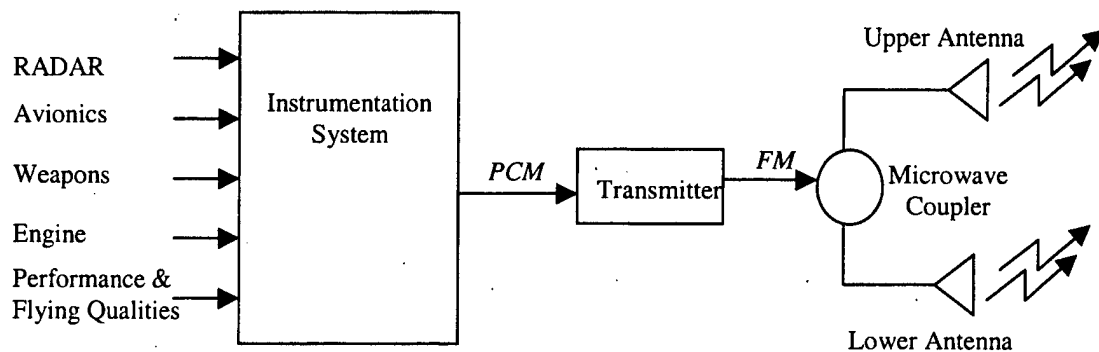


Figure 3-6: Instrumentation system typical of a flight test aircraft

When the instrumentation system is installed in the aircraft, quite frequently there is no analysis performed concerning the effective radiation pattern of the telemetry antenna. More often, the placement of the antenna is chosen based on installations accomplished in the past. If ever an analysis had been performed to determine the effective radiation pattern of a telemetry antenna on a particular type of aircraft, the information is not currently documented. It is the intent of the following simulation to ascertain the performance of a 2.25 GHz telemetry antenna on an F-18 aircraft.

The model of the F-18 aircraft is shown in Figure 3.7. Three locations are considered as shown in the figure. With the telemetry antenna (see Figure 2-5) located at A, APATCH produced data for the three planes of interest (roll, pitch, and yaw) as shown in Figure 3-8.

The roll plane pattern (Figure 3-8a) shows the directive gain. Unlike the case of the C-172 with the quarter-wave vertical element, it is necessary to examine both the E_θ and E_ϕ

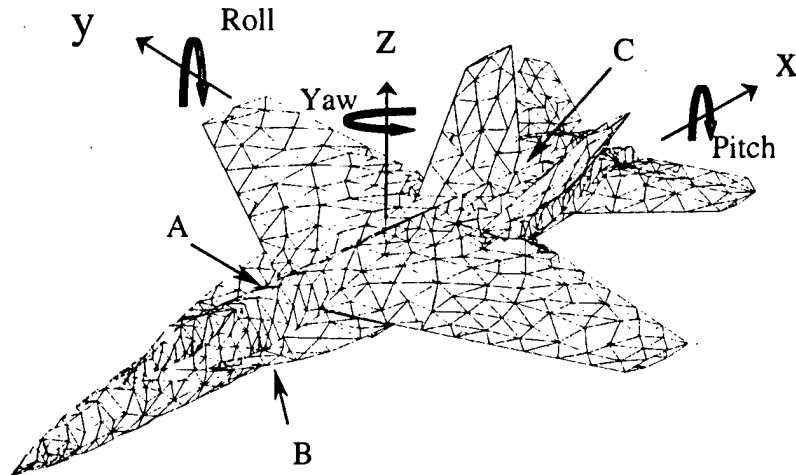


Figure 3-7: ACAD model of F-18 Hornet. Locations where the telemetry antenna was considered are designated A,B, and C.

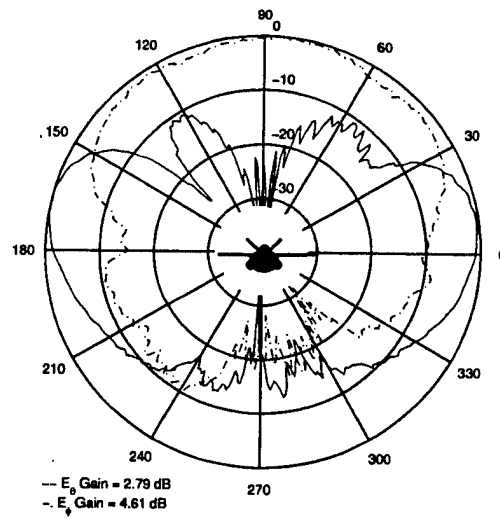
polarizations. Since the radiating element in the telemetry antenna is canted rearward at a 45° angle with respect to the specified coordinate system, the E_ϕ polarization will become significant at various observation angles and must be considered in the ensuing analysis. One sees that there is good coverage above the aircraft due to the E_ϕ polarization. Below the aircraft, however, there is reduced coverage, as one might expect. The net decrease in gain below the aircraft is greater than 30 dB from the maximum occurring above the aircraft.

Figure 3-8b shows the pitch plane pattern for the antenna at location A. This plot shows good coverage in the region above the aircraft but decreased performance below. Only the E_θ polarization is shown because the E_ϕ polarization, being on the order of 20 dB below the E_θ polarization, was not considered significant in this plane.

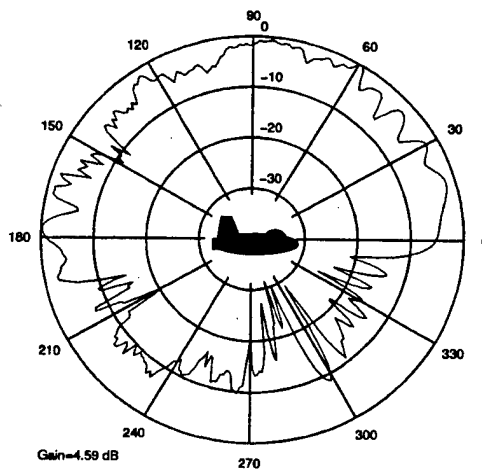
The yaw plane is shown in Figure 3-8c. One concludes from this plot that there is uniform coverage around the horizontal plane of the aircraft. There are some variations in the pattern at observation angles coincident with the nose and tail, but they do not seem to be very large and would probably not significantly degrade the overall performance of the telemetry system.

The E_ϕ polarization is shown as the broken line. At 0° and 180° , the E_ϕ pattern exhibits a deep null. This is due to the fact that from these observation points, the field is entirely θ polarized. However, at 90° and 270° , the magnitude of E_ϕ is at or near its maximum. From these angles, the cant of the antenna results in a non-zero ϕ component to the electric field.

(a)



(b)



(c)

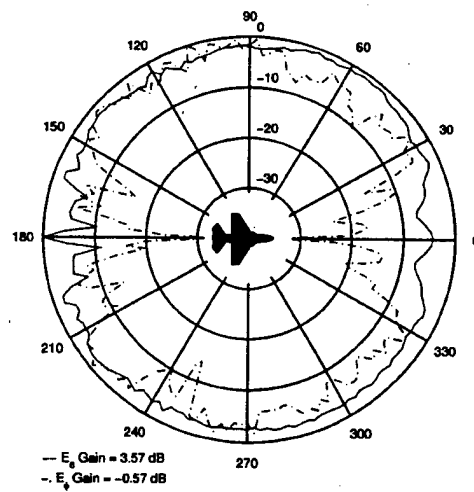


Figure 3-8: F-18 with 2.25 GHz telemetry antenna at location A. E_0 (solid line), E_ϕ (broken line); (a) roll, (b) pitch and (c) yaw

When the telemetry antenna is located at B, the plots of Figure 3-9 result. Referring to the roll plane pattern, (Figure 3-9a) when E_θ and E_ϕ polarizations are considered, good reception can be expected from the lower mounted antenna in the roll plane.

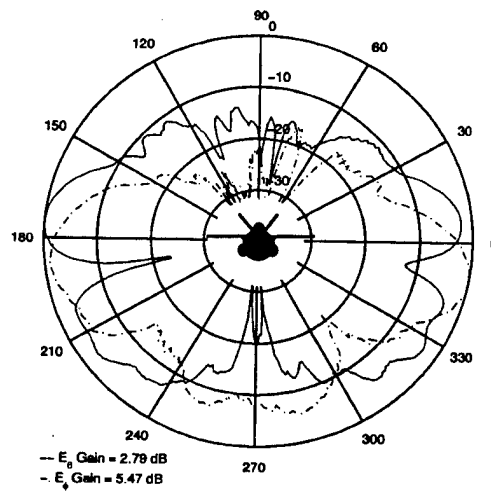
Figure 3-9b shows the pitch plane pattern. The upper region of the plot indicates poor radiation from the lower antenna, as one might expect. Alternatively, the telemetry antenna does a good job of radiating into the space below the aircraft. While it is difficult to attribute the nulls in the pattern between the angles of 180° and 260° to a specific area of the aircraft, it is, nevertheless, indicative of the multi-path effect that is occurring in this region.

The yaw plane pattern is shown in Figure 3-9c. It is very similar to the corresponding pattern for location A. The gain is about 1.7 dB lower than the gain for location A.

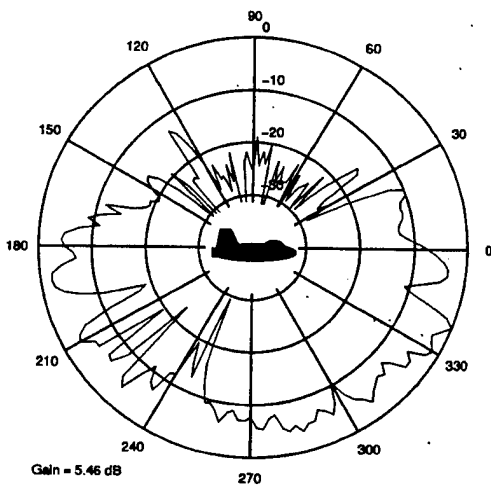
It can be concluded from the foregoing analysis that good performance can be expected when the antenna is installed at locations A or B. When it is installed at A, the antenna radiates well into the region above the aircraft, and when it is located at B, it transmits well into the space below the aircraft. The type of test mission being conducted dictates whether to install the antenna on the top of the aircraft or the bottom. An aircraft conducting tests at low altitudes (for example, a terrain-following mission) requires a top-mounted antenna. The telemetry is transmitted from this antenna to a second aircraft flying at a high altitude that serves as an airborne mission control or a relay to a test control facility located on the ground. On the other hand, an aircraft flying at high altitudes (such as a bomber conducting weapons tests) would probably utilize a lower-mounted antenna and transmit directly to a ground station.

With a highly dynamic aircraft such as the F-18, it is more likely to use two antennas, one on the bottom and one on top. This approach ensures that there is adequate telemetry reception to the ground station as the aircraft executes the maneuvers required for a particular test. As shown in Figure 3-6, the two antennas are connected to the transmitter by a microwave coupler. The coupler divides the input signal into two equal-phase signals to be directed to the telemetry antennas. Often, the coupler is of a type that divides the power into two equal signals, a 3 dB coupler. However, there are times when the coupler divides the power so that 10% of the input power is directed to the upper antenna and 90% to the lower antenna, a 10 dB coupler. This is done for a majority of tests since the underside of the aircraft is exposed to the ground station receiving the telemetry. The upper antenna is supplied so that the telemetry link is maintained during the brief time that a maneuver is executed, albeit the power from this antenna is significantly reduced. The ensuing analysis considers both cases. That is, an upper antenna and a lower antenna used simultaneously with either a 3 dB or a 10 dB coupler.

(a)



(b)



(c)

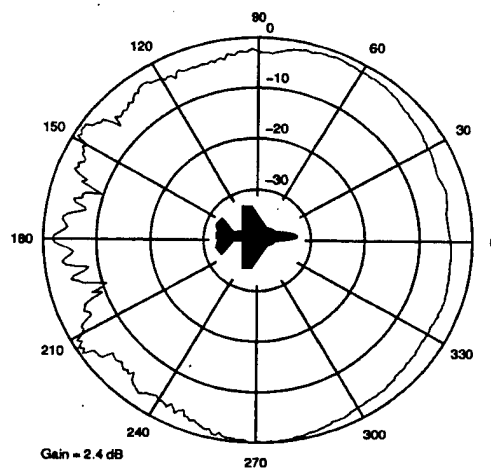


Figure 3-9: F18 with 2.25 GHz telemetry antenna at location B. E_θ (solid line), E_ϕ (broken line), (a) roll, (b) pitch and (c) yaw

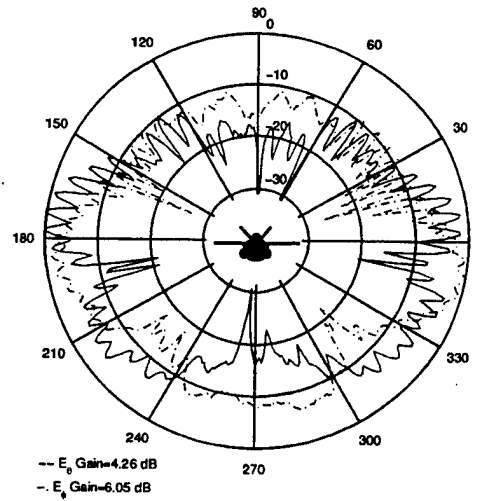
APATCH results are shown in Figure 3-10 for the 10 dB coupler. The roll plane pattern (Figure 3-10a) shows the E_θ and E_ϕ polarizations. It can be seen that good coverage in the lower region can be expected. The region above the aircraft exhibits lower radiation levels than in the region below the aircraft; this is expected when the 10 dB coupler is used. The pitch plane is shown in Figure 3-10b. It is very similar to the corresponding plot for the case when only the single lower antenna is used (see Figure 3-9), except that there is slightly more radiation into the space above the aircraft. Finally, the yaw plane pattern is shown in Figure 3-10c. This plot shows the interference pattern resulting from the use of the two antennas.

When a 3 dB coupler is used with the instrumentation system, the effective radiation patterns from the upper and lower telemetry antenna are shown in Figure 3-11. The roll and pitch plane patterns indicate that there is satisfactory radiation into the regions above and below the aircraft. This is the type of coverage desired when the aircraft is performing test missions requiring frequent maneuvers and unusual attitudes like those encountered in flutter and high-alpha testing.

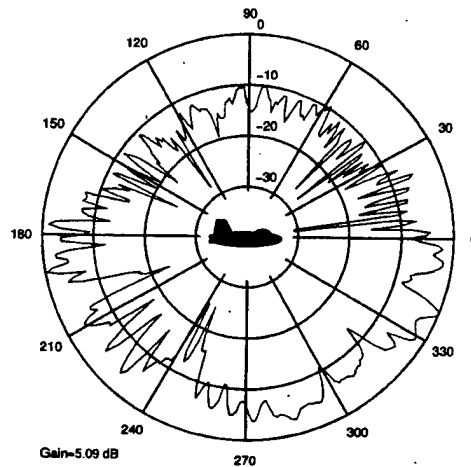
The yaw plane pattern shown in Figure 3-11c is quite interesting. Dramatic variations in the E_θ and E_ϕ polarizations are evident as the observation angle varies in the horizontal plane. It should be noted that the peaks and nulls of the two polarizations seem to occur in an alternating fashion. This is an interferometer type of effect due to the horizontal separation of the antennas, which is 6.55λ . The oscillations in the magnitude of each polarization arise from the path length difference to an observation point from each antenna. When this difference is a multiple of one-half wavelength, then a null is observed in the pattern (destructive interference). A peak results when the path length difference is a multiple of one wavelength (constructive interference). The onset of this phenomenon is also apparent in Figure 3-10c when the 10 dB coupler is used, although, its effect is not as pronounced as observed with the 3 dB coupler.

With regard to the overall performance of the instrumentation system, the peaks and nulls in the yaw plane do not affect the reception of the telemetry signal at the ground station. Generally, the ground station employs a circularly polarized antenna that results in a 3 dB loss. [1] On the other hand, this oscillatory behavior in the pattern can be misleading to engineers and technicians troubleshooting the aircraft. Quite often, a vertically polarized antenna is used in a mobile trailer that is positioned alongside the aircraft to check the telemetry system prior to a test flight. If the trailer is positioned in a location corresponding to one of the nulls in the E_θ pattern, poor signal quality would be received at the mobile trailer possibly leading to a drop-out of the telemetry system. The instrumentation engineer might be led into thinking that a problem exists

(a)



(b)



(c)

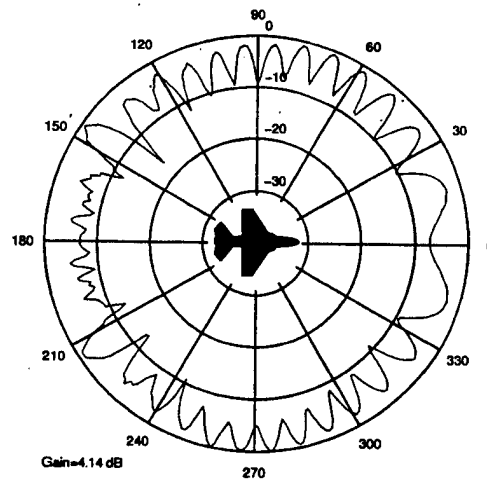
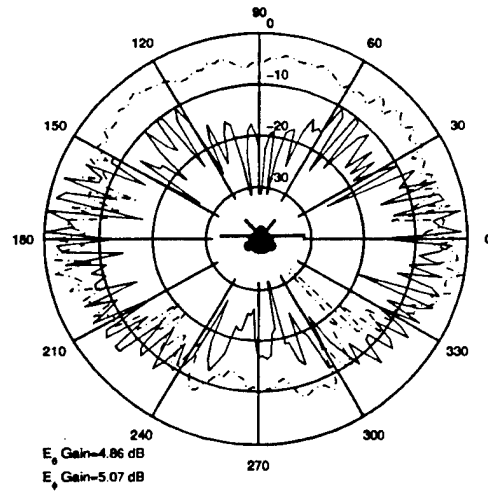
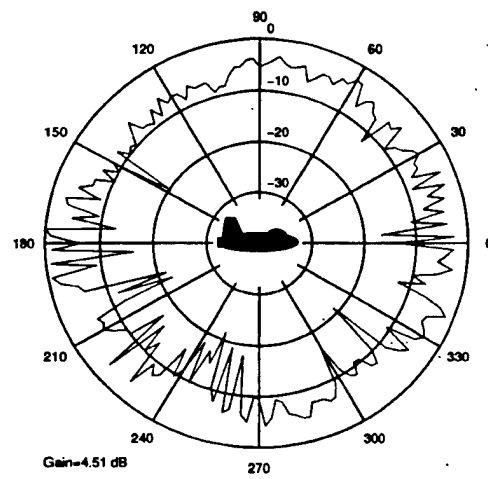


Figure 3-10: F-18 with two 2.25 GHz telemetry antennas and a 10 dB microwave coupler. E_θ (solid line), E_ϕ (broken line), (a) roll, (b) pitch and (c) yaw

(a)



(b)



(c)

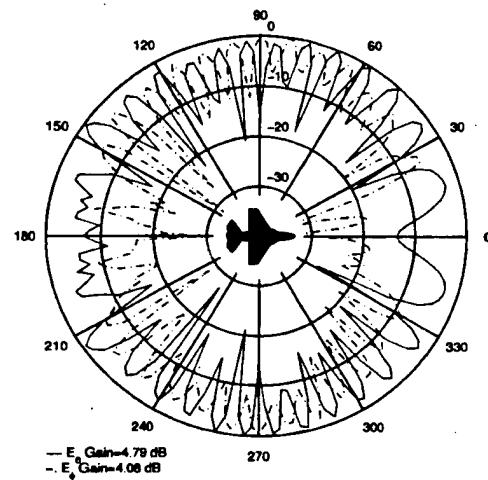
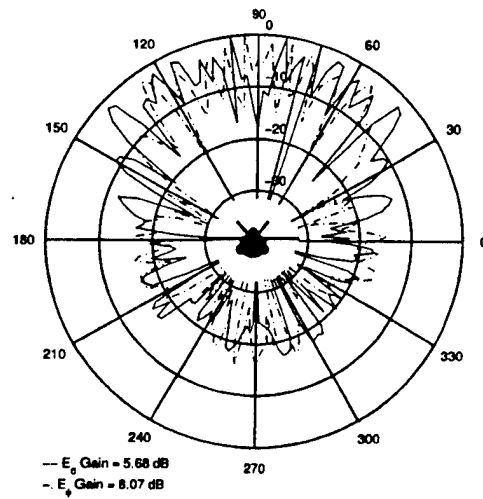


Figure 3-11: F-18 with two 2.25 GHz telemetry antennas and a 3 dB microwave coupler.
 E_θ (solid line), E_ϕ (broken line), (a) roll, (b) pitch and (c) yaw

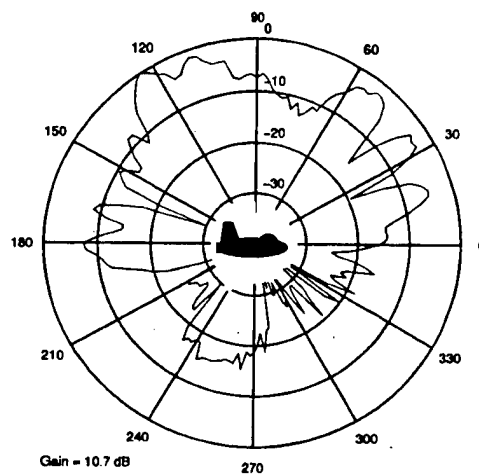
with the telemetry system and cancel the scheduled mission. The cost incurred to test programs as a consequence of cancellations of this type can be quite prohibitive.

Strictly as a point of curiosity, the antenna was placed at location C. In practice, this location is not suitable for an antenna installation due to the proximity of the engines resulting in additional maintenance actions. Furthermore, as one might intuitively point out, the field-of-view is reduced due to the presence of the canted twin tails. Nevertheless, the APATCH results for this configuration are shown in Figure 3-12. Immediately, the poor performance of the antenna at this location is evident. The roll plane pattern shows dramatic oscillations in the gain above the aircraft while the pitch plane seems to favor radiation only into a selected range of angles ($\sim 30^\circ$, 60° , and 120°). The blockage from the vertical tails of the aircraft in the yaw plane can be seen in Figure 3-12c. Radiation is concentrated forward and aft of the aircraft, but it is greatly hindered to the sides as a consequence of the blockage from the canted twin tails of the aircraft.

(a)



(b)



(c)

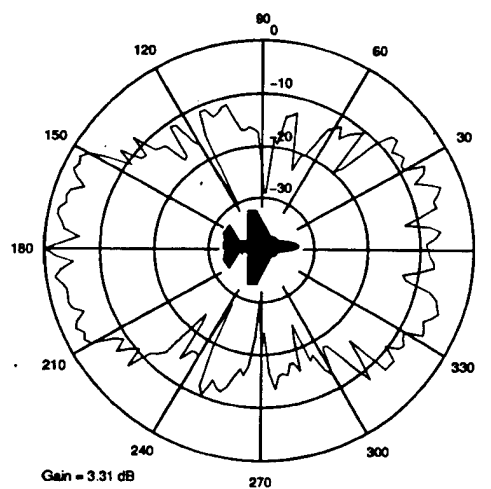


Figure 3-12: F-18 with 2.25 GHz telemetry antenna at location C.
 E_0 (solid line), E_ϕ (broken line), (a) roll, (b) pitch and (c) yaw

IV. SUMMARY AND CONCLUSIONS

This study analyzed the performance of low-gain antennas installed on aircraft. Chapter II presented a brief review of scattering mechanisms and relevant electromagnetic theory. It also described the operation of APATCH and the implementation of the SBR method. To validate the use of APATCH, the program was used to compute the radiation pattern of a 2.25 GHz telemetry antenna installed on a cylinder, for which measured data was available. From this, it was learned how to best model the telemetry antenna within the APATCH computer program. The chapter also included the results from PATCH, an electromagnetics code based on the method of moments.

Chapter III began with an analysis of the performance of a quarter-wavelength (1030 MHz) monopole antenna on a C-172 aircraft. APATCH computed the effective radiation pattern for the antenna at two locations. The analysis also considered a two-element array, which was found to be more suitable for the TCAS application since it afforded a greater field-of-view in the forward direction. This is where TCAS coverage is most essential.

The third chapter concluded with a study of the radiation patterns of a 2.25 GHz telemetry antenna installed on an F-18 aircraft. APATCH provided the radiation patterns for the antenna installed on the top and the bottom of the aircraft. Often, the instrumentation system utilizes two telemetry antennas simultaneously to provide coverage as the aircraft executes maneuvers during a flight test. APATCH computed the radiation pattern for this situation as well. When the 3 dB coupler was considered, an interference pattern resulted in the yaw plane which could present problems during the pre-flight checks of the aircraft telemetry system.

Since APATCH is relatively easy to use, the analysis of many aircraft/antenna systems is conveniently afforded. Suggestions for further study include the behavior of GPS and other avionics systems on the aircraft. Of further interest is the performance of EW pods located on wing stations. The presence of external stores and large aircraft components, such as the wings and fuselage, greatly affect the radiation pattern of the antennas located on the EW pods. The difficulty in this type of study exists with the use of the ACAD program and the availability of aircraft computer models. ACAD is not an intuitive program, but requires specialized training to learn how to construct even the most simple of shapes and structures. A large selection of ACAD aircraft models is not readily available, but models can be constructed from accurate drawings of the aircraft, once the operation of the ACAD program has been mastered.

LIST OF REFERENCES

1. Balanis, Constantine A., *Antenna Theory, Analysis and Design*, John Wiley and Sons, New York, NY, 1982
2. Skolnik, Merrill I., *Introduction to Radar Systems*, McGraw-Hill, Inc., New York, NY, 1980
3. Grudzinski, Sigmund S., "Development of B-1 Antenna Measurement Test Bed," *IEEE AES Systems Magazine*, April 1991
4. Jenn, David C., *Radar and Laser Cross Section Engineering*, American Institute of Aeronautics and Astronautics, Inc., Washington, DC, 1995
5. Cheng, David K., *Field and Wave Electromagnetics*, 2nd edition, Addison-Wesley Publishing Company, Reading, MA, 1989
6. Jenn, David C., "Performance Evaluation of Antennas Installed on a Joint Stand-Off Weapons (JSOW) Captive Air Training Missile (CATM)," NPS Research Report, NPS-EC-98-008, March 10, 1998
7. Balanis, Constantine A., *Advanced Engineering Electromagnetics*, John Wiley and Sons, Inc., New York, NY, 1989
8. Ozdemir, T., Nurnberger, M. W., Volakis, J. L., Kipp, R., Berrie, J., "A Hybridization of Finite-Element and High-Frequency Methods for Pattern Predictions for Antennas on Aircraft Structures," *IEEE Antennas and Propagation Magazine*, Vol. 38, No. 3, June 1996
9. Baldauf, John, Lee, Shung-Wu, Lin, Luke, Jeng, Shyh-Kang, Scarborough, Steven M., Yu, C. L., "High Frequency Scattering from Trihedral Corner Reflectors and Other Benchmark Targets: SBR Versus Experiment," *IEEE Transactions on Antennas and Propagation*, Vol. 39, No. 9, September 1991
10. Ling, Hao, Chou, Ri-Chee, Lee, Shung-Wu, "Shooting and Bouncing Rays: Calculating the RCS of an Arbitrarily Shaped Cavity," *IEEE Transactions on Antennas and Propagation*, Vol. 37, No. 2, February 1989
11. Marzougui, Adel M., Franke, Steven J., "Scattering from Rough Surfaces Using the Shooting and Bouncing Rays (SBR) Technique and Comparison with the Method of Moments Solutions," *IEEE Antennas and Propagation International Symposium*, 1990, Vol. 4, pg 1540-1543
12. *ACAD Users Manual*, Lockheed-Martin, Fort Worth, TX, 76108
13. *APATCH Ver 2.1 Users Manual*, DEMACO Inc., 100 Trade Center Drive, Champaign, IL, 61820
14. "TCAS—The Complete Heads Up," Product Support News, Winter 1998, [<http://www.raytheon.com/rac/suppnews/jet/tcas.htm>]

INITIAL DISTRIBUTION LIST

	No. of Copies
1. Defense Technical Information Center..... 8725 John J. Kingman Rd., STE 0944 Ft. Belvoir, Virginia 22060-6218	2
2. Dudley Knox Library..... Naval Postgraduate School 411 Dyer Rd. Monterey, California 93943-5101	2
3. Chairman, Code EC..... Department of Electrical and Computer Engineering Naval Postgraduate School Monterey, California 93943-5101	1
4. Professor David C. Jenn, Code EC/Jn..... Department of Electrical and Computer Engineering Naval Postgraduate School Monterey, California 93943-5101	2
5. Professor John P. Powers, Code EC/Po..... Department of Electrical and Computer Engineering Naval Postgraduate School Monterey, California 93943-5101	1
6. Robert Kipp..... DEMACO, Inc. 100 Trade Center Drive, Suite 303 Champaign, IL 61820	1
7. Stassi Cramm..... 412 TW/EWE 195 E. Popson Edwards AFB, CA 93523	1
8. Pete Burke..... 412 TW/EWE 195 E. Popson Edwards AFB, CA 93523	1
9. James Calusdian..... 43851 Amy Ct Lancaster, CA 93535	2